

Research Article

Xenogenic Esophagus Scaffolds Fixed with Several Agents: Comparative *In Vivo* Study of Rejection and Inflammation

Holger Koch,¹ Cora Graneist,¹ Frank Emmrich,^{1,2} Holger Till,³ Roman Metzger,³ Heike Aupperle,⁴ Katrin Schierle,⁵ Ulrich Sack,^{1,2} and Andreas Boldt^{1,2}

¹ Translational Centre for Regenerative Medicine (TRM), University of Leipzig, 04103 Leipzig, Germany

² Institute of Clinical Immunology, Faculty of Medicine, University of Leipzig, 04103 Leipzig, Germany

³ Department of Pediatric Surgery, University of Leipzig, 04103 Leipzig, Germany

⁴ Institute of Pathology, Faculty of Veterinary Medicine, University of Leipzig, 04103 Leipzig, Germany

⁵ Institute of Pathology, University of Leipzig, 04103 Leipzig, Germany

Correspondence should be addressed to Holger Koch, holger.koch@trm.uni-leipzig.de

Received 27 September 2011; Revised 14 December 2011; Accepted 15 December 2011

Academic Editor: George E. Plopper

Copyright © 2012 Holger Koch et al. This is an open access article distributed under the Creative Commons Attribution License, which permits unrestricted use, distribution, and reproduction in any medium, provided the original work is properly cited.

Most infants with long-gap esophageal atresia receive an esophageal replacement with tissue from stomach or colon, because the native esophagus is too short for true primary repair. Tissue-engineered esophageal conducts could present an attractive alternative. In this paper, circular decellularized porcine esophageal scaffold tissues were implanted subcutaneously into Sprague-Dawley rats. Depending on scaffold cross-linking with genipin, glutaraldehyde, and carbodiimide (untreated scaffolds : positive control; bovine pericardium : gold standard), the number of infiltrating fibroblasts, lymphocytes, macrophages, giant cells, and capillaries was determined to quantify the host response after 1, 9, and 30 days. Decellularized esophagus scaffolds were shown to maintain native matrix morphology and extracellular matrix composition. Typical inflammatory reactions were observed in all implants; however, the cellular infiltration was reduced in the genipin group. We conclude that genipin is the most efficient and best tolerated cross-linking agent to attenuate inflammation and to improve the integration of esophageal scaffolds into its surrounding tissue after implantation.

1. Introduction

Pediatric tissue engineering is subjected to special requirements: the scaffolds need to be suitable for and adapted to mechanical and biological changes during childhood [1]. As recently described, different types of scaffold materials such as hydrogels, synthetic, or natural scaffolds have already been studied in tissue engineering, for example, long-gap esophageal atresia [2–5]. In general, natural scaffolds possess several advantages compared to other models. Decellularized extracellular matrix (ECM) scaffolds can easily be obtained from donors (humans or animals). All cellular components can be removed from the scaffolds by the use of chemical, biological, or mechanical methods and allowing an off-the-shelf production [6]. ECM scaffolds are rich in structural proteins and have an intact three-dimensional structure [7]. By removing cells and cellular antigens, the ECM

scaffolds are obviously biocompatible and are thought not to provoke a chronic rejection reaction after implantation into another species. However, ECM proteins can also provide costimulatory signals to immune cells [7–12]. Therefore, inflammatory reactions and remodeling and degradation processes cannot be excluded. The degree of inflammation or remodeling is strongly dependent on the scaffold material and chemical treatment, so-called cross-linking [6, 7, 13–16]. It is supposed that native scaffolds are subjected to fast enzymatic degradation in the recipient's body, accompanied by the loss of mechanical properties. On the one hand, degradation is necessary for the development of a constructive remodeling process. However, on the other hand, after scaffold implantation *in vivo*, it needs to maintain its mechanical properties and the scaffold should be used as a matrix for reseeding by different tissue-typical cells. After successful in-growth by, for example, muscle cells

or fibroblasts, remodeling processes in the scaffold will occur according to the new biological environment (e.g., the subcutaneous region). A compromise has to be effected to lower the rate of degradation (without completely blocking), downregulate inflammation, and to increase the rate of cellular infiltration. Both depend strongly on the biological properties of the scaffold. A common approach for increasing the mechanical strength, inhibiting inflammatory processes, and decreasing the rate of degradation of biologic scaffolds is the use of chemical cross-linking agents.

The common principle of cross-linking is based on the presumption that free amino ($-\text{NH}_2$), carboxyl ($-\text{COOH}$), and hydroxyl groups ($-\text{OH}$) on collagen may have antigenic effects. These free groups were cross-linked and masked with appropriate chemical reagents such as glutaraldehyde, genipin, or carbodiimides. Some cross-linking agents are toxic (e.g., formalin) or tend to calcificate the implant (e.g., glutaraldehyde (GA)); others have been described to be well tolerated (e.g., genipin (GP)) or to be metabolized residue-free in the cross-linking reaction (e.g., carbodiimide (CDI)) [17–19].

In the present study, we investigated in an animal model whether an acellular esophagus provokes an inflammatory response, rejection or is well tolerated. In detail, we implanted small circular pieces of esophagus scaffolds into rats subcutaneously. We used chemically pretreated (cross-linked) and untreated scaffolds. Chemically pre-treated scaffolds were cross-linked either with GA, GP, or CDI. As control, commercially available bovine pericardium (BP; St. Jude, USA; cross-linked with glutaraldehyde) was used. Furthermore, the polarization of macrophages is important to the remodeling outcome and was therefore investigated. M1-activated macrophages express IL-12^{high}, IL-23^{high}, IL-10^{low} and produce inflammatory cytokines such as IL-1 β , IL-6, and TNF- α , which promote active inflammation. They are inducer and effector cells in Th1-type inflammatory responses [20] and express CCR7 as a surface cell marker [6, 21]. In contrast, M2-activated macrophages have an IL-12^{low}, IL-23^{low} and IL10^{high} phenotype and are able to facilitate tissue repair and constructive remodeling [20, 22, 23]. M2 macrophages predominantly induce the Th2 response, which is particularly beneficial for the constructive tissue remodeling. In addition, macrophages of anti-inflammatory phenotype inhibit proinflammatory cytokines and express the surface marker CD163 [15, 20, 24, 25]. Macrophages are able to change their polarization in response to local stimuli during the process of wound healing [26]. The recognition of the predominant phenotype of macrophages provides an indication of scaffold rejection, inflammation or acceptance after implantation. However, the anti-inflammatory phenotype may be simultaneously detected with the general macrophage marker CD68 by immunohistochemical methods [27]. Furthermore, the general macrophage marker CD68 also stains pro-inflammatory and not activated or polarized macrophages. Therefore, the CD163/CD68 ratio can be used to calculate the amount of M2 macrophages over time.

Thus, the objective of this work was to characterize the host response to different cross-linked ECM esophageal

scaffolds, in particular aspects of inflammation or rejection and the macrophage polarization to clarify the most suitable cross-linking agent for the integration of ECM esophageal scaffolds into its surrounding tissue after implantation.

2. Methods

2.1. Porcine Esophagus Scaffold. All experiments were performed with esophagi of pigs (*Deutsche Landrasse*, 25–65 kg) in cooperation with the Heart Center Leipzig, Department of Cardiac Surgery. The organs were obtained under sterile conditions and stored at 4°C in a 0.9% NaCl solution.

For decellularization, esophagi were cut into pieces of 8 cm length, and the tunica adventitia was removed mechanically. Esophagi were then placed in a 5% sodium dodecyl sulfate-solution (SDS; Roth, Karlsruhe, Germany) for 7 days. After complete removal of all cells, the scaffolds were washed in phosphate buffered saline (PBS) for 2 days. After finishing the decellularization, the tissue was digested enzymatically by adding DNase (200 $\mu\text{g}/\text{mL}$; Sigma, Deisenhofen, Germany) in PBS + MgCl_2 (50 mM) and incubated in 37°C for 12 h. After washing in PBS, the scaffolds were sterilized by gamma radiation (25 kGy from a ⁶⁰Co source) and stored in PBS at 4°C for maximum 4 weeks.

2.2. Histology. Following decellularization and after explantation at day 1, 9, and 30 postimplantation, scaffolds were fixed in paraformaldehyde solution. Representative areas were embedded in paraffin wax, cut into slices (5 μm thickness), and routinely stained by Azan and HE staining [28]. In Azan stained slides, the matrix morphology of decellularized porcine scaffolds was compared to that of native esophagi using light microscopy. The assessment of HE-stained neutrophils, fibroblasts, giant cells, and microvessels were performed by light microscopy on explanted scaffolds. Cells were scored as follows: 0 = no cells; 1 = 1–100 cells; 2 \geq 100–200 cells; 3 \geq 200 cells/5 mm².

2.3. Immunohistochemistry. Immunohistochemical analysis of decellularized esophagus was performed with a commercially available Envision DAB staining kit (DAKO, Carpinteria, USA). Briefly, formalin-fixed, paraffin-embedded esophagus tissue sections of 5 μm thickness were deparaffinized. Subsequently, slices were heated in 50 mM Tris buffered saline solution at 95°C for 15 min. After cooling, the slides were incubated with proteinase K (250 $\mu\text{g}/\text{mL}$) for 10 min and washed in distilled water. Endogenous enzyme activity was blocked (10 min, DAKO staining kit), and the tissue slides were incubated with primary antibodies. The staining steps with anti-collagen III (Acris Antibodies, Herford, Germany), anti-collagen IV (Acris Antibodies), anti-fibronectin (Dianova, Berlin, Germany), and anti-elastin (Acris Antibodies) were performed following the manufactures instruction (Envision DAB Staining Kit, DAKO). The specificity was controlled by omitting the primary antibodies. All antibodies were diluted 1:100 in PBS. In stained slices, extracellular matrix composition of decellularized and native scaffolds was investigated by light microscopy.

TABLE 1: Group composition with type and cross-linking of scaffolds.

Group	<i>n</i>	Type of scaffold	Scaffold cross-linking
untreated	9	decellularized, sterilized esophagus scaffold	untreated
GA	9	decellularized, sterilized esophagus scaffold	glutaraldehyde
GP	9	decellularized, sterilized esophagus scaffold	genipin
CDI	9	decellularized, sterilized esophagus scaffold	carbodiimide
BP (control)	9	decellularized, sterilized bovine pericard scaffold	glutaraldehyde (bovine pericardium; St. Jude, USA)
sham (negative control)	15	—	—

To investigate cellular infiltration in explanted scaffolds, the following antibodies were used: anti-CD3, anti-CD68, anti-CD163 (all Serotec, Oxford, UK), and anti-hydroxyl-prolyl-hydrogenase (hPH, BMA Biomedical, Augst, Switzerland). All antibodies were diluted 1:50 in PBS. Control experiments were carried out without primary antibodies. To visualize the nuclei, all slices were counterstained with Mayer's hemalun solution. In stained slices, from each section, the CD3, CD68, and CD163 positive cells as well as nuclei were counted in 3×5 microscopic fields by two blinded observers (magnification $\times 1000$). The data are represented as a ratio of CD-positive cells/nuclei (mean \pm standard error of mean (SEM)).

2.4. DNA Quantification in Decellularized Matrix Scaffolds. The isolation and quantification of DNA in the decellularized tissue scaffolds was performed using the protocol of Qiagen (DNeasy, Hilden, Germany). In brief, decellularized esophagus matrix scaffolds were cut into small cross-sectional pieces of 25 mg. Lysis buffer and proteinase K (Qiagen, Hilden, Germany) were added, and samples were incubated overnight in a shaking water bath (56°C). After successful tissue lysis, the DNA was purified and measured spectrophotometrically using a Nanodrop Spectrophotometer (Peqlab, Erlangen, Germany). The DNA-content of matrix scaffolds undergoing enzymatic digestion was compared to matrix scaffolds without enzymatic digestion (both $n = 6$). Native esophagus tissue served as positive control ($n = 6$).

2.5. Cross-Linking of Esophagus Scaffolds. For carbodiimide cross-linking, circular pieces of esophagus scaffolds (3 mm thickness) were immersed in 2-(N-morpholino)ethanesulfonic acid buffer (MES buffer; 0.2 M, pH 5.0; Sigma, Munich, Germany). After 1 h, the MES buffer was discarded and the scaffolds were incubated in a solution consisting of MES buffer (0.2 M, pH 5.0), N-hydroxysuccinimide (NHS; 0.12 M), and N-(3-dimethylaminopropyl)-N-ethylcarbodiimide (EDC; 0.3 M). After 16 h, the scaffolds were removed and rinsed in MES buffer for 24 h and in PBS for at least 24 h [17, 29]. For GP cross-linking, the scaffolds were incubated in a 0.33% genipin/ethanol solution (Alexis, Lausen, Switzerland) for 3 days at 37°C. Then the scaffolds were removed and rinsed in 75% ethanol for 2 h and in PBS for 3 days [21, 30, 31]. For glutaraldehyde cross-linking, the scaffolds were immersed in 0.625% glutaraldehyde/distilled

water (Sigma) for 3 days at 37°C. Subsequently, the scaffolds were removed and washed in PBS for 3 days [32].

2.6. Subcutaneous Rat Model. 60 Sprague-Dawley rats were grouped according to scaffold cross-linking: untreated, GA, GP, CDI, BP, and sham group (each treatment group: $n = 9$; sham group: $n = 15$; for details see Table 1). Each rat of the treatment groups received a piece of scaffold subcutaneously. Animals of the sham group underwent the same surgical procedure but received no implants.

Before subcutaneous implantation of scaffolds, the animals were anesthetized with 0.15 mg/kg medetomidin (Pfizer, Berlin, Germany), 2 mg/kg midazolam (Ratiopharm, Ulm, Germany), and 0.005 mg/kg fentanyl (Janssen-Cilag, Neuss, Germany). After 15 min, circular pieces of cell-free esophagus scaffolds (3 mm thickness) were implanted into a subcutaneous back pocket of the rat (1 cm length). The wound was sewn with two stitches. Finally, the anesthesia was antagonized with 0.75 mg/kg atipamezol (Pfizer), 0.2 mg/kg flumazenil (Roche, Penzberg, Germany), and 0.12 mg/kg naloxon (Ratiopharm). All surgical interventions were performed under sterile conditions. For possible emerging pain the rats were given carprofen (5 mg/kg s.c., Pfizer) postoperative for 3 days.

After postoperative care for 1, 9, and 30 days, the animals were narcotized, euthanized, and the scaffolds were explanted. Tissue was immersed in 4% paraformaldehyde solution and embedded in paraffin for further histological investigations (see above). All procedures were approved by the committee of Animal Care and Use of the relevant local governmental body (TVV03/09) in accordance to the law of experimental animal protection. All efforts were made to minimize the number of animals used.

2.7. Statistics. The statistical evaluation of the immunohistology was performed by Kruskal-Wallis with post hoc Mann-U-Whitney. Effect of decellularization on the DNA-content was evaluated using a one-way ANOVA, followed by post hoc Tukey test for pairwise comparisons. Values of $P < 0.05$ were considered statistically significant. Furthermore, the lower and upper 95% confidence intervals (CI) were measured for the calculation of an area, where the true value is of a probability of at least 95%. Differences were considered significant if the lower and the upper CI among two groups did not overlap.

3. Results

3.1. Porcine Esophagus Scaffold. To investigate whether the ECM composition of the decellularized esophagus scaffold (Figure 1(a); top) is similar to native esophagus tissue (Figure 1(a); bottom), both tissues were histologically and immunohistologically characterized. Azan staining of natural (Figure 1(b)) and acellular esophagus scaffolds (Figure 1(c)) revealed anatomical intact structures, optimal matrix geometry, and no remaining cellular structures. As demonstrated in Figure 2, collagen III (Figure 2(a)) and fibronectin (Figure 2(b)) could be observed in large amounts in all tissue areas (submucosa, muscular layer) in acellular similar to natural esophagi (small pictures, Figures 2(a)–2(d)). The vessels expressed collagen IV (Figure 2(c)) and elastin, which is additionally located in tela submucosa (Figure 2(d)).

3.2. DNA Quantification. A one-way ANOVA revealed a significant effect of decellularization on the DNA-content compared to controls [$F_{(2,15)} = 15.918$; $P < 0.001$]. The remaining DNA in the decellularized matrix scaffolds undergoing DNA digestion was 8.05 ± 2.01 ng/mg versus 756.96 ± 49.07 ng/mg in control tissues (native esophagus; $n = 6$). The DNA content of decellularized matrix scaffolds without nucleic acid digestion was 10.04 ± 3.01 ng/mg ($n = 6$), see Figure 3. The post hoc comparison did not reveal significant differences in the remaining DNA content of decellularized scaffolds with and without DNA digestion ($P = 0.757$). The percentage of remaining DNA content after both procedures was decreased by about 99% compared with native esophagus tissue ($P < 0.001$; without digestion: $98.7 \pm 0.4\%$, respectively, with digestion: $98.9 \pm 0.3\%$).

3.3. Response to Implanted Decellularized Esophagus Scaffolds. A set of representative pictures of cell infiltration into untreated (Figures 4(a)–4(c)) and cross-linked scaffolds (GP, Figures 4(d)–4(f)) is shown in Figure 4. At day 1 postimplantation, untreated scaffolds (Figure 4(a)) displayed a cellular infiltration from the periphery to the center of the tissue. In GP cross-linked scaffolds (Figure 4(d)), only a cellular layer was detectable at the periphery. At day 9 postimplantation, an increase of infiltrating cells into untreated scaffolds (Figure 4(b)) was observed compared to GP cross-linked (Figure 4(e)) scaffolds. At day 30 postimplantation, whole implants of the untreated scaffold group (Figure 4(c)) were infiltrated with cells, whereas GP scaffolds (Figure 4(f)) showed only an immaterial cellular infiltration. Furthermore, in all cross-linked groups (GP, GA, CDI, BP) the infiltrating rate was decreased compared to the untreated scaffold group. Differences among GP, GA, CDI, and BP could not be observed. In addition, untreated scaffolds were degraded largely compared to cross-linked scaffolds at day 30 postimplantation. Furthermore, all scaffolds were infiltrated with granulocytes migrating from the periphery to the central region at day 1 postimplantation, without detecting any differences among the groups. Single lymphocytes were seen.

At day 9, the number of granulocytes decreased and macrophages, fibroblasts, and lymphocytes appeared. They also migrated from the periphery to the center of the tissue. In terms of chronic-granulating inflammation, capillary growth reached a maximum. Among the groups, no significant differences were detected.

At day 30, scaffolds were infiltrated by fibroblasts and sporadically by lymphocytes or granulocytes. In terms of chronic-granulating inflammation, collagen fibers and macrophages were increased accompanied by decreased amount of capillaries. All data are summarized in Figure 5.

For detailed analysis of infiltration of macrophages, lymphocytes, and fibroblasts, scaffold slides were stained immunohistologically with anti-CD3, anti-CD68, anti-CD163, and anti-hPH antibodies. For estimating the effects, the data of BP, GP, GA, and CDI were compared to those of the untreated group. At day 1, no CD3-, CD163-, or hPH-positive cells were detected in any scaffold. Scaffold analysis at day 9 revealed a significantly lower number of CD163 macrophages in BP, whereas at day 30 in BP, GP, GA, and CDI CD163 macrophages were significantly decreased as compared to the untreated group (Figure 6(a)). Also, at day 9 only in the BP group CD68-positive cells were observed to a significantly lesser extent. However, at day 30, CD68-positive cells were also significantly decreased in the GP group (Figure 6(b)). Additionally, in most groups the amount of anti-inflammatory, proremodeling macrophage M2 phenotype increased from day 9 to day 30, indicated by a higher CD163/CD68 ratio (untreated: + 26.88%; BP: + 82.14%; GP: + 23.51%), except the GA (–28.65%) and CDI (–74.79%) group (Figure 6(c)). Analysis of CD3-positive lymphocytes reveals in all groups only a marginal infiltration into the scaffold. The percentage was less than 0.5%, and no significant differences between the groups were detected (not shown). Immunohistological hPH staining demonstrated a tendency to increase in number of fibroblasts in the GA and GP groups at day 9. At day 30, in the GP and CDI group, the numbers of fibroblasts were significantly increased compared to the untreated group (Figure 6(d)).

4. Discussion

Xenogenic biological ECM scaffolds are widely used in tissue engineering for regenerative medicine. These scaffolds have the advantage of possessing intact structural proteins and growth factors that reduce inflammatory responses [33–36]. The response of the host to several xenogenic ECM scaffolds has been well characterized and understood; however, it is only partially studied in animal models for esophageal cross-linked ECM scaffolds [7–13, 22, 24, 25, 35–41]. Additionally, previously published data suggest that the host response to the ECM scaffolds is strongly dependent on the species and chemical pretreatment [15, 42]. Therefore, currently published data are not universally valid.

Thus, it is essential to find out the host response after subcutaneous implantation of porcine esophagus scaffolds. Furthermore, the outcome of the host response after implantation of different cross-linked ECM scaffolds was studied.

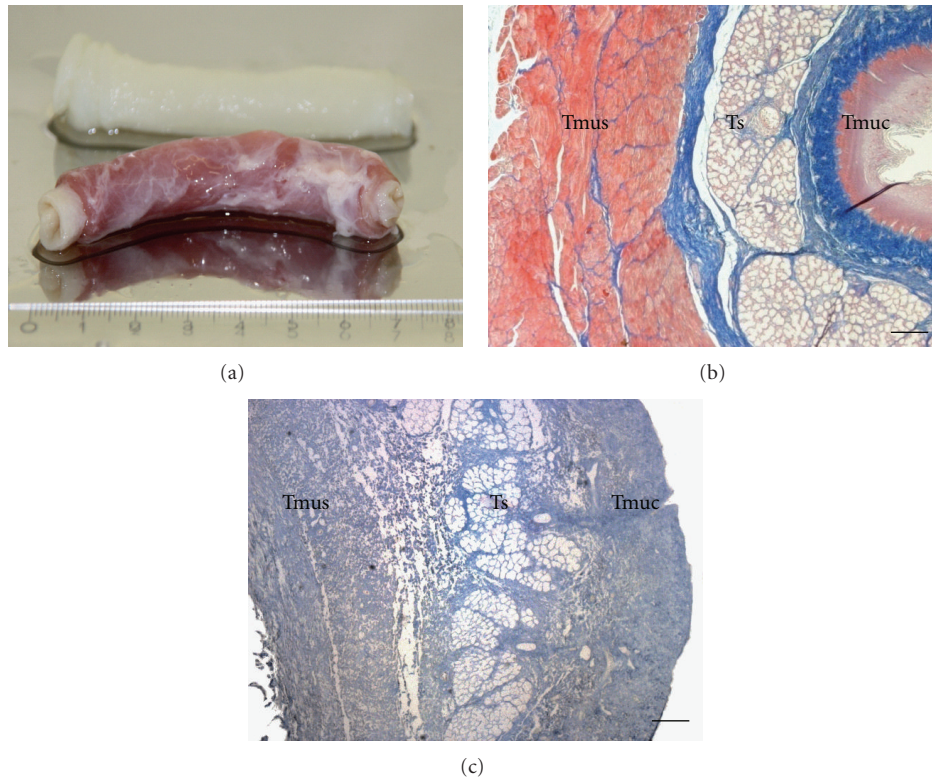


FIGURE 1: A representative piece of esophagus before (bottom) and after (top) decellularization (a). (b) and (c) show the tissue morphology before (b) and after decellularization (c) of porcine esophagus. Acellular esophagus scaffolds showed anatomical intact structures, optimal matrix geometry, and no remaining cellular structures. Connective tissue was stained blue, chromatin red, muscle cells orange, and erythrocytes red. Magnification: $\times 40$, bar = $100 \mu\text{m}$. Tmus: Tunica muscularis; Ts: Tela submucosa; Tmuc: Tunica mucosa.

Since the scaffolds were decellularized and morphologically intact, we assume that a chronic rejection will not occur. This is not common, because in studies with small intestinal submucosa (SIS)-ECM T-lymphocyte infiltrations, encapsulations and necrosis were observed as signs of rejection [13, 14]. In the present study, only in one animal, encapsulation was observed at day 9 postimplantation. None of the used scaffolds showed signs of necrosis or T-cell infiltration ($\text{CD}3 \leq 0.5\%$).

Nevertheless, the implanted xenogenic esophagus scaffolds provoked inflammatory reactions. Signs of inflammation were granulocyte infiltration at day 1, encapsulation by macrophages and fibroblasts at day 9, and scaffold infiltration of macrophages and fibroblasts at day 30 postimplantation. This is characteristic for structural remodeling processes such as scarring after foreign body implantation and was consistent with our expectations. We do not assume that DNA remnants of the scaffolds were the cause of inflammatory reactions in our experiment, though in the recent literature such a reaction was described. In most biological material, remaining DNA consisted of fragments less than 300 bp. The remnant DNA is subject to fast enzymatic degradation *in vivo* [15, 43]. Instead of remnant DNA as cause of inflammation, it is more plausible that free amino ($-\text{NH}_2$), carboxyl ($-\text{COOH}$), and hydroxyl ($-\text{OH}$) groups of the remaining collagen scaffold may be

responsible for the immunological reactions [18, 44]. To avoid or inhibit such reactions, these free groups can be bound by functional groups of chemical cross-linking, which precludes the antigenic properties of collagen [17, 18, 45]. In the present study, the scaffolds were pretreated by three different cross-linking agents: CDI, GA, and GP. The cross-linkers were selected in accordance with descriptions of the biological compatibility in the recent literature [18, 34].

An alternative to the use of GA and GP may be the application of CDI. First, CDI reacts with the free carboxyl- followed by the amine groups of collagen, generating the cross-link and representing a treatment method without residual chemicals [17, 18]. By fixation with CDI, tissue quality was improved, the grade of calcification was lowered (compared to GA), and no toxicity was observed [18]. CDI was also used as a cross-linking agent in commercially available tissue products [15]. Nevertheless, in the present study a fixation of the esophagus scaffolds with CDI did not indicate the expected results. Unfortunately, in the CDI group, the $\text{CD}163/\text{CD}68$ ratio was decreased at day 30 postimplantation, indicating a switch to a proinflammatory and destructive M1 macrophage phenotype. In contrast to GA and GP fixed tissue as well as to untreated scaffolds, we observed a chronic inflammation, which was maintained and increased after the CDI cross-link. One might speculate that this effect might be caused by incomplete fixation.

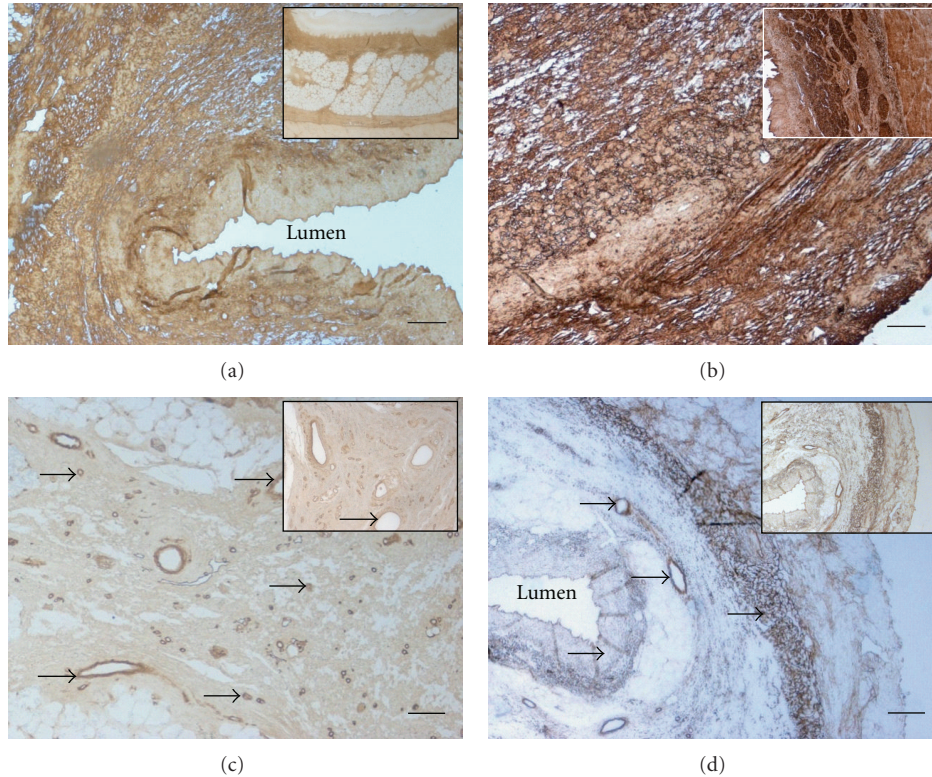


FIGURE 2: Immunohistochemical DAB staining (brown staining) of decellularized porcine esophagus tissue for collagen III (a), fibronectin (b), collagen IV (c), and elastin (d) in comparison to natural esophagus (small pictures). The arrow heads mark vessels. Decellularized esophagus scaffolds were shown to maintain native extracellular matrix composition. Original magnification: x40 (a and d) and x100 (b and c); bar = 100 μm .

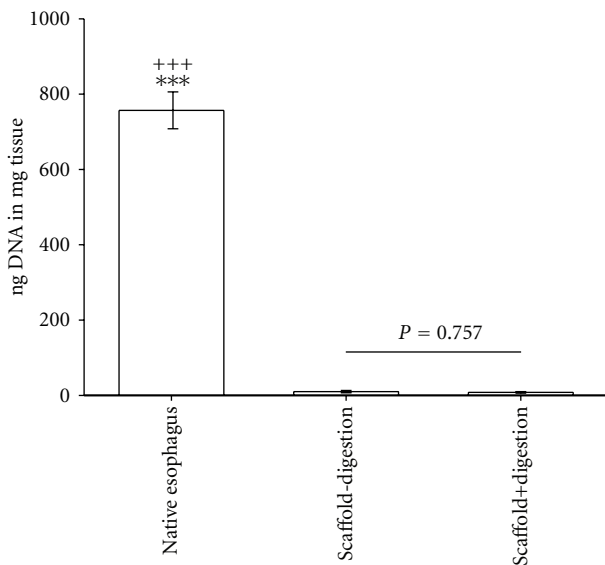


FIGURE 3: The comparison of remaining DNA content in decellularized esophageal tissue with and without DNA digestion (both $n = 6$). Significant differences between both groups do not exist ($P = \text{n.s.}$). Native, untreated esophageal tissue served as control ($n = 6$). *** = $P < 0.001$ versus decellularized esophagus without DNA digestion group. +++ = $P < 0.001$ versus decellularized esophagus with DNA digestion group.

Interestingly, other studies described similar effects in CDI-fixed SIS-ECM tissue [15, 46]. After implantation of CDI-fixed SIS-ECM, Badylak and colleagues could also observe a predominant M1 macrophage phenotype, characterized by chronic inflammation at week 16 postimplantation [46]. Furthermore, it is reported that CDI cross-linking caused a decrease in elasticity and mechanical toughness [47], which is essential for esophageal function. On the basis of these data, CDI cannot be considered as an optimal cross-linker in the present study.

GA is the most common cross-linking agent and often used in commercially available tissues [15]. Tissue that is cross-linked with GA exhibits a decreased immunological reaction and stabilized collagen scaffold [41, 48, 49]. We also observed that the immunological response in GA cross-linked esophagus scaffolds was lower in comparison to chemically untreated scaffolds. At day 30 postimplantation, the rate of CD163 macrophages was decreased, but the total number of macrophages (CD68) remained constant [15, 20, 24, 40]. Interestingly, in contrast to GP, BP, and the untreated scaffold group, CD163/CD68 ratio was decreased at day 30 postimplantation. This might indicate a switch to a proinflammatory and destructive M1 macrophage phenotype. An increase of T-lymphocyte infiltration could not be observed. However, the suppression of immunological actions of xenografts by GA is not complete; cellular toxicity

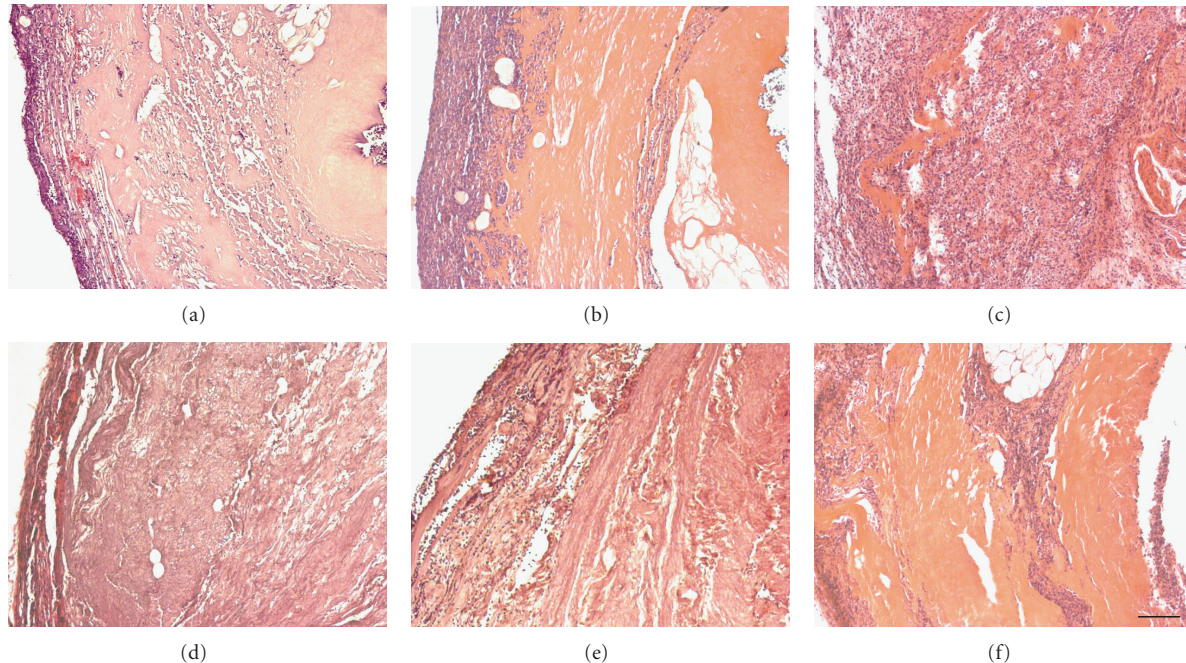


FIGURE 4: Transverse section of subcutaneous untreated (a–c) and GP cross-linked (d–f) implants after 1, 9, and 30 days *in vivo*. At day 1 postimplantation, untreated scaffolds (a) displayed a cellular infiltration with granulocytes, fibroblasts, and macrophages, whereas in GP cross-linked scaffolds (d) only a cellular layer was detectable at the periphery. At day 9 postimplantation, a considerable increase of infiltrating cells into untreated scaffolds (b) was detected as a sign of encapsulation, whereas GP cross-linked (e) scaffolds showed a cellular infiltration with granulocytes, fibroblasts, and macrophages without signs of encapsulation. At day 30 postimplantation, whole implants of the untreated scaffold group (c) were infiltrated with granulocytes, fibroblasts, and macrophages, whereas GP cross-linked scaffolds (f) showed only an immaterial cellular infiltration. In contrast to GP cross-linked scaffolds, untreated scaffolds were largely degraded. See Figure 5 for detailed cellular analysis. Magnification: $\times 100$, bar = 100 μm . HE-staining.

and host immune response (cytotoxic T-cell activation) have been described [21, 35, 37, 45]. Furthermore, cytotoxicity of GA cross-linked bioprostheses for host fibrocytes, fibroblasts, and macrophages has been described [50, 51]. In the present study, we did not observe any cytotoxic effect of GA cross-linked esophagus scaffolds on host fibroblasts or macrophages compared to the untreated group. However, the use of GA as a cross-linker to reduce the inflammatory response comprises further disadvantages. Depolymerization of GA cross-links as well as calcification of implants has been reported [18]. However, in our study, we did not find signs of calcification and the process of depolymerization was not investigated. The sum of our data suggests that GA was not an optimal cross-linker for constructive remodeling in the present study (e.g., CD68+macrophage infiltration), which corresponds with other disadvantages described in the literature [35, 37, 50, 51].

A naturally occurring cross-linking agent is GP. It reacts with collagen amino groups and is approximately 10,000 times less cytotoxic than GA [21, 34, 45]. It forms stable cross-linking products, reacts antiphlogistically, protects against inflammatory degradation, and causes faster tissue regeneration in comparison to GA [30, 39, 52]. An *in vitro* degradation assay demonstrated that GP-fixed acellular scaffold tissue kept burst pressures equivalent to GA cross-linked scaffold tissue [34]. Furthermore, recent

literature showed that proliferative capacity of infiltrated cells was greater than that after GA cross-linking [31, 34]. In *in vivo* experiments in dogs, decreased inflammation around implanted GP-fixed acellular arteries was observed compared to GA-fixed implants; however, the degree of inflammation has not been clearly described [22]. Signs of calcification were not detected in GP-fixed tissue [19, 45]. These results correspond to findings of our studies. In an *in vivo* experiment in rats, a minimal macrophage infiltration or localization outside untreated and treated scaffolds was observed at day 30 postimplantation [34]. However, in a study that compared the host inflammatory response to subcutaneously implanted GP and GA cross-linked acellular bovine pericardia, the cross-linking with GA caused a significantly increased inflammatory response compared to untreated and GP cross-linked tissue scaffolds [21]. We could show that macrophages were present in untreated and cross-linked scaffolds at day 1 postimplantation. However, at day 30 postimplantation, pretreatment with GP caused a significant decrease of infiltrating macrophages (compared to untreated scaffolds). Moreover, immunohistochemical staining revealed that pan-macrophage marker CD68 were significantly decreased in GP, similar to the reference scaffold BP (compared to untreated scaffolds). In scaffolds treated with GA or CDI, a decrease of CD68 macrophages could

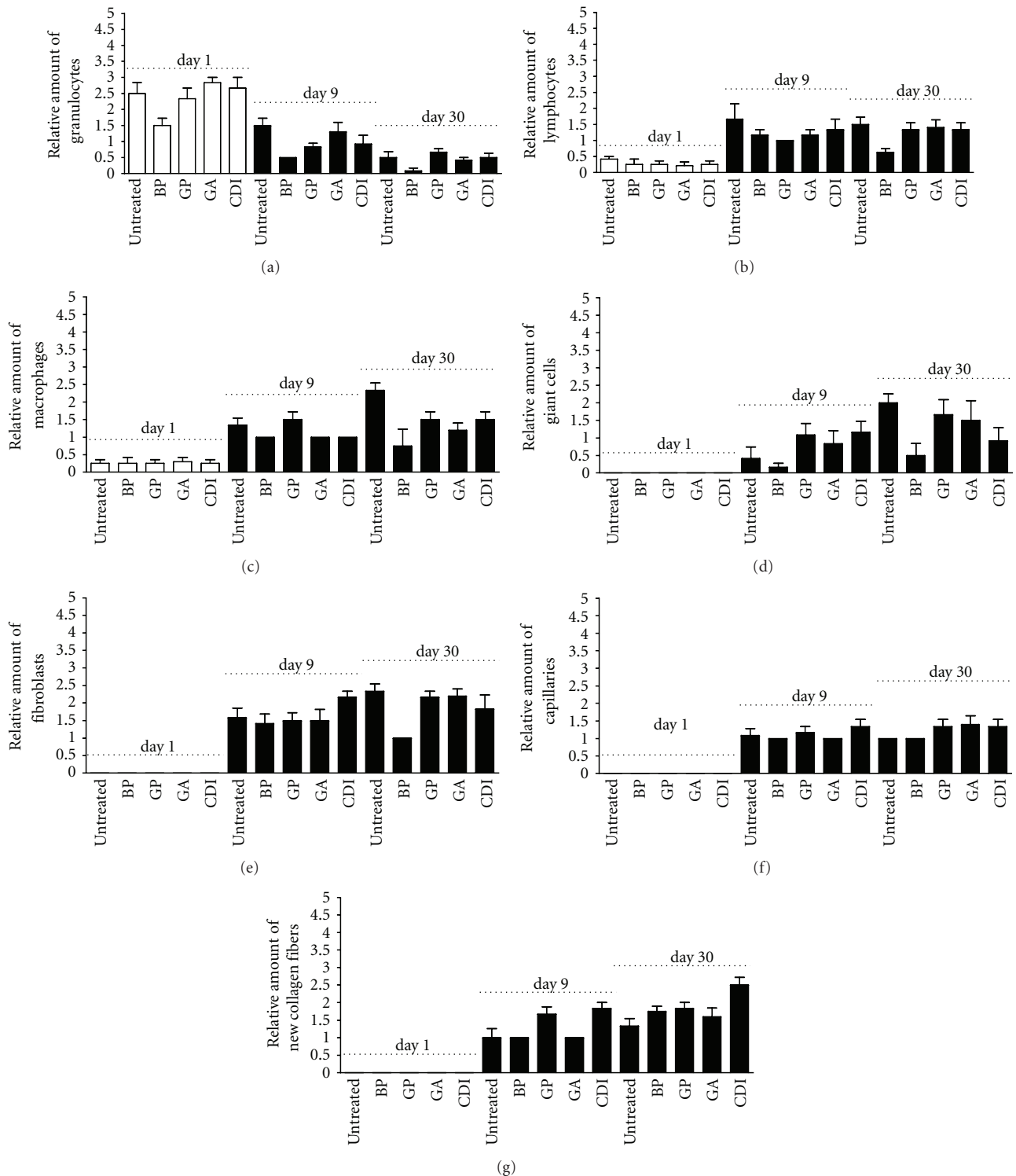


FIGURE 5: HE-staining analysis of the degree of scaffold infiltration by granulocytes (a), lymphocytes (b), macrophages (c), giant cells (d), fibroblasts (e), capillaries (f), and collagen fibers (g) after 1, 9, and 30 days. In all implants, an increase of infiltration by lymphocytes, macrophages, giant cells, fibroblasts, capillaries, and collagen fibers could be observed at day 30 compared to day 1 postimplantation. Furthermore, a decrease of infiltrating granulocytes could be observed in all implants at day 30 compared to day 1 postimplantation. Data were calculated based on the scoring by two blinded pathologists ($n = 3$ per group and day; one field per slide and rat; each 5 mm^2): 1 = 1–100 cells; $2 \geq 100$ –200 cells; $3 \geq 200$ cells. “-”: untreated scaffold; BP: bovine pericardium (St. Jude, USA); GP: genipin; GA: glutaraldehyde; CDI: carbodiimide. Differences did not reach the level of significance.

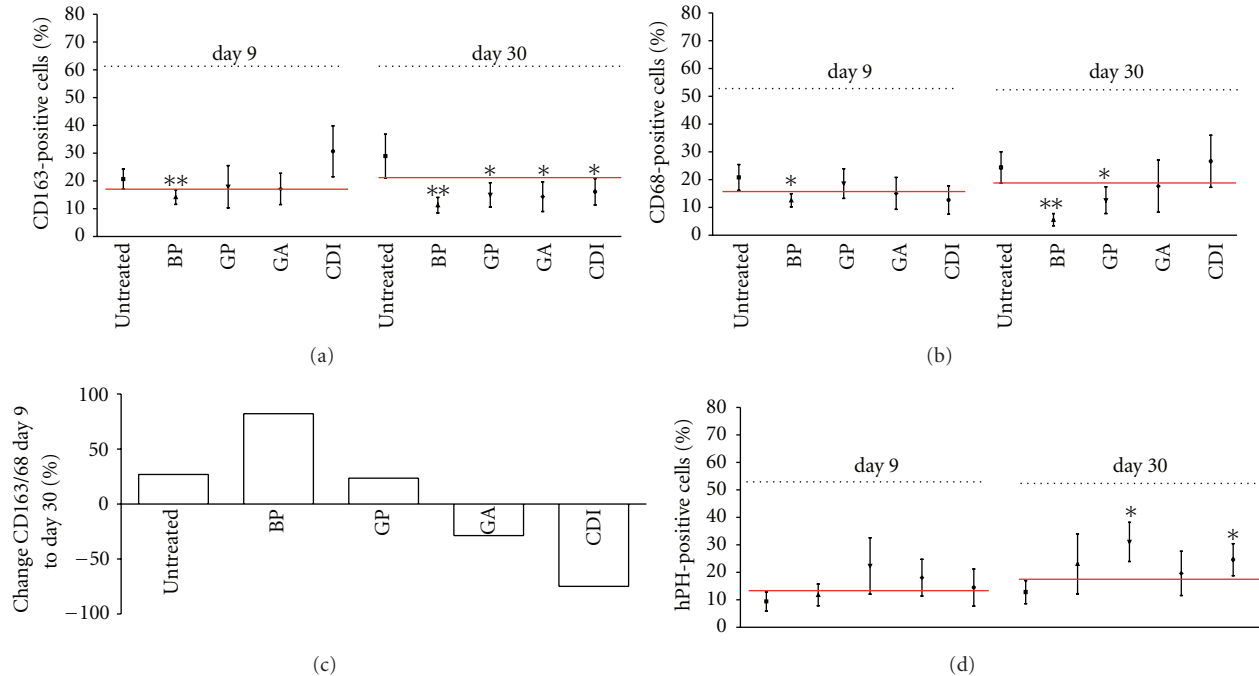


FIGURE 6: Immunohistological analysis of the degree of scaffold infiltration by CD163 (a), CD68 (b), and hPH-positive fibroblasts (d) after 9 and 30 days, as well as the CD163/CD68 ratio (c). At day 30 postimplantation, a decrease of infiltrating CD163-positive macrophages could be observed in all implants compared to untreated scaffolds. Furthermore, a decrease of infiltrating CD68+macrophages could be observed in the BP group, as well as after cross-linking with GP compared to untreated scaffolds at day 30. Untreated and cross-linked scaffolds, except the CDI and GA groups, showed a macrophage M2 phenotype switch at day 30 postimplantation, indicated by a positive CD163/CD68 ratio at day 30 compared to ratio at day 9. All data were represented as ratios of specific cells/total cells \pm SEM. Five microscopic fields (magnification $\times 1000$) of one slide per rat were analyzed ($n = 3$ per group and day). An average of 75 ± 2.15 total cells per microscopic field was counted to generate the ratio of cells/total cells. All implants were compared by means and confidence interval to the untreated implant. Differences were considered as significant if confidence intervals do not overlap or by $P < 0.05$, see red line. Untreated: untreated scaffold; BP: bovine pericardium (St. Jude, USA); GP: genipin; GA: glutaraldehyde; CDI: carbodiimide; hPH: hydroxyl-prolyl-hydroxylase. * $P < 0.05$, ** = $P < 0.01$ versus untreated decellularized esophagus tissue.

not be observed and the macrophage infiltration remained unchanged on a high level. One might assume that GP prevented scaffolds from inflammation processes in contrast to CDI or GA or untreated scaffolds.

In addition, we calculated the CD163/CD68 ratio to define the change in the amount of the proremodeling M2 macrophages over time. At day 30 postimplantation, we detected an M2 macrophage phenotype switch, which is known to be associated with constructive remodeling and tissue repair [20, 22, 23], whereas in GA and CDI cross-linked scaffolds a destructive M1 macrophage phenotype was detected. Furthermore, GP-fixed scaffolds exhibited a moderate degradation, extremely low lymphocyte infiltration and a significantly increased fibroblast infiltration compared to untreated scaffolds. The presence of proremodeling macrophages and fibroblasts (which are some of the typical cells in the subcutaneous region) cells might be suggestive of host repair and constructive tissue remodeling [23, 53]. Furthermore, the infiltration, survival, and living of the tissue-fibroblasts suggested a biocompatibility of GP scaffolds.

5. Conclusion

The present subcutaneous rat model proved to be an appropriate experimental tool to investigate the influence of different cross-linking agents on host response (after implantation of porcine ECM scaffolds) and to identify the best tolerated cross-linking agent. Signs of graft rejection such as encapsulation or lymphocyte infiltration did not occur in any group. However, differences in inflammatory processes and infiltration of cells such as macrophages or fibroblasts could be observed depending on scaffold pretreatment with different crosslinking agents. High rates of proinflammatory macrophages were detected in untreated, CDI, and GA scaffolds. This indicated inflammatory processes resulting in fast scaffold degradation and a low rate of integration of the scaffold in the surrounding tissue. In contrast, scaffolds treated with GP were only mildly infiltrated by macrophages (CD68), similar to the established reference standard BP. Moreover, in GP, the proinflammatory CD163 macrophage phenotype was significantly decreased, lymphocytes were at the limit of detection, and the rate of subcutaneous tissue-typical fibroblasts was increased. This

might suggest that GP was an agent that scaffolds prevented for graft rejection and is efficient to attenuate inflammatory processes. Low rates of macrophages and infiltration of fibroblasts (in the subcutaneous region) in GP scaffolds imply a better scaffold tolerance and an improved integration of esophageal scaffolds into their surrounding tissue after implantation. This suggested the practicability of GP as a cross-linking agent for implants in clinical application [32]. We consider GP an adequate compromise between the rate of degradation, inflammation, and the infiltration by tissue typical cells.

The results of the present study help to provide a new piece of the puzzle in the development of esophageal xenografts. The use of acellular esophagus scaffolds could be an important therapeutic tool in the near future. The development of a large animal model seems to be the next step to prove the functionality and host response (constructive remodeling processes) after the implantation of segmental GP cross-linked ECM esophagus scaffolds in the esophageal location. If this approach is successful, there is a wide range of applications possible (e.g., esophagus atresia, esophageal trauma, long-segment Barrett's esophagus, etc.) to increase the quality of life of patients and minimize the complications in severe esophageal diseases.

Conflicts of Interests

The authors confirm that all authors have read and approved the paper and that there are no conflicts of interest.

Acknowledgments

The work presented in this paper was made possible by funding from the German Federal Ministry of Education and Research (BMBF, PtJ-Bio, 0318853). Special thanks are due to Bettina Glatte, Ramona Blaschke, and Ina Görz for excellent laboratory work.

References

- [1] M. Patel and J. P. Fisher, "Biomaterial scaffolds in pediatric tissue engineering," *Pediatric Research*, vol. 63, no. 5, pp. 497–501, 2008.
- [2] G. S. Arul and D. H. Parikh, "Oesophageal replacement in children," *Annals of the Royal College of Surgeons of England*, vol. 90, no. 1, pp. 7–12, 2008.
- [3] J. E. Foker, B. C. Linden, E. M. Boyle, and C. Marquardt, "Development of a true primary repair for the full spectrum of esophageal atresia," *Annals of Surgery*, vol. 226, no. 4, pp. 533–543, 1997.
- [4] L. Spitz, "Oesophageal atresia," *Orphanet Journal of Rare Diseases*, vol. 2, no. 1, article 24, 2007.
- [5] H. Till, O. J. Muensterer, U. Rolle, and J. Foker, "Staged esophageal lengthening with internal and subsequent external traction sutures leads to primary repair of an ultralong gap esophageal atresia with upper pouch tracheoesophageal fistula," *Journal of Pediatric Surgery*, vol. 43, no. 6, pp. E33–E35, 2008.
- [6] T. W. Gilbert, T. L. Sellaro, and S. F. Badylak, "Decellularization of tissues and organs," *Biomaterials*, vol. 27, no. 19, pp. 3675–3683, 2006.
- [7] S. F. Badylak, "Xenogeneic extracellular matrix as a scaffold for tissue reconstruction," *Transplant Immunology*, vol. 12, no. 3–4, pp. 367–377, 2004.
- [8] T. L. Adair-Kirk and R. M. Senior, "Fragments of extracellular matrix as mediators of inflammation," *International Journal of Biochemistry and Cell Biology*, vol. 40, no. 6–7, pp. 1101–1110, 2008.
- [9] K. Z. Konakci, B. Bohle, R. Blumer et al., "Alpha-Gal on bioprosthesis: Xenograft immune response in cardiac surgery," *European Journal of Clinical Investigation*, vol. 35, no. 1, pp. 17–23, 2005.
- [10] O. Lider, R. Hershkoviz, and S. G. Kachalsky, "Interactions of migrating T lymphocytes, inflammatory mediators, and the extracellular matrix," *Critical Reviews in Immunology*, vol. 15, no. 3–4, pp. 271–283, 1995.
- [11] S. R. Morwood and L. B. Nicholson, "Modulation of the immune response by extracellular matrix proteins," *Archivum Immunologiae et Therapiae Experimentalis*, vol. 54, no. 6, pp. 367–374, 2006.
- [12] M. Tanemura, D. Yin, A. S. Chong, and U. Galili, "Differential immune responses to α -gal epitopes on xenografts and allografts: implications for accommodation in xenotransplantation," *Journal of Clinical Investigation*, vol. 105, no. 3, pp. 301–310, 2000.
- [13] A. J. Allman, T. B. McPherson, S. F. Badylak et al., "Xenogeneic extracellular matrix grafts elicit a Th2-restricted immune response," *Transplantation*, vol. 71, no. 11, pp. 1631–1640, 2001.
- [14] A. J. Allman, T. B. McPherson, L. C. Merrill, S. F. Badylak, and D. W. Metzger, "The Th2-restricted immune response to xenogeneic small intestinal submucosa does not influence systemic protective immunity to viral and bacterial pathogens," *Tissue Engineering*, vol. 8, no. 1, pp. 53–62, 2002.
- [15] S. F. Badylak and T. W. Gilbert, "Immune response to biologic scaffold materials," *Seminars in Immunology*, vol. 20, no. 2, pp. 109–116, 2008.
- [16] J. E. Valentin, J. S. Badylak, G. P. McCabe, and S. F. Badylak, "Extracellular matrix bioscaffolds for orthopaedic applications: a comparative histologic study," *Journal of Bone and Joint Surgery - Series A*, vol. 88, no. 12, pp. 2673–2686, 2006.
- [17] F. Everaerts, M. Torrianni, M. Hendriks, and J. Feijen, "Biomechanical properties of carbodiimide crosslinked collagen: influence of the formation of ester crosslinks," *Journal of Biomedical Materials Research Part A*, vol. 85, no. 2, pp. 547–555, 2008.
- [18] E. Khor, "Methods for the treatment of collagenous tissues for bioprosthesis," *Biomaterials*, vol. 18, no. 2, pp. 95–105, 1997.
- [19] H. W. Sung, Y. Chang, C. T. Chiu, C. N. Chen, and H. C. Liang, "Cross-linking characteristics and mechanical properties of a bovine pericardium fixed with a naturally occurring cross-linking agent," *Journal of Biomedical Materials Research*, vol. 47, no. 2, pp. 116–126, 1999.
- [20] A. Mantovani, A. Sica, and M. Locati, "Macrophage polarization comes of age," *Immunity*, vol. 23, no. 4, pp. 344–346, 2005.
- [21] Y. Chang, C. C. Tsai, H. C. Liang, and H. W. Sung, "In vivo evaluation of cellular and acellular bovine pericardium fixed with a naturally occurring crosslinking agent (genipin)," *Biomaterials*, vol. 23, no. 12, pp. 2447–2457, 2002.
- [22] B. N. Brown, J. E. Valentin, A. M. Stewart-Akers, G. P. McCabe, and S. F. Badylak, "Macrophage phenotype and remodeling outcomes in response to biologic scaffolds with and without a cellular component," *Biomaterials*, vol. 30, no. 8, pp. 1482–1491, 2009.

- [23] L. Chin, A. Calabro, E. R. Rodriguez, C. D. Tan, E. Walker, and K. A. Derwin, "Characterization of and host response to tyramine substituted-hyaluronan enriched fascia extracellular matrix," *Journal of Materials Science*, vol. 22, no. 6, pp. 1465–1477, 2011.
- [24] A. Mantovani, A. Sica, S. Sozzani, P. Allavena, A. Vecchi, and M. Locati, "The chemokine system in diverse forms of macrophage activation and polarization," *Trends in Immunology*, vol. 25, no. 12, pp. 677–686, 2004.
- [25] F. O. Martinez, A. Sica, A. Mantovani, and M. Locati, "Macrophage activation and polarization," *Frontiers in Bioscience*, vol. 13, no. 2, pp. 453–461, 2008.
- [26] R. D. Stout and J. Suttles, "Immunosenescence and macrophage functional plasticity: dysregulation of macrophage function by age-associated microenvironmental changes," *Immunological Reviews*, vol. 205, pp. 60–71, 2005.
- [27] T. Kushiyama, T. Oda, M. Yamada et al., "Alteration in the phenotype of macrophages in the repair of renal interstitial fibrosis in mice," *Nephrology*, vol. 16, no. 5, pp. 522–535, 2011.
- [28] A. Boldt, A. Scholl, J. Garbade et al., "ACE-inhibitor treatment attenuates atrial structural remodeling in patients with lone chronic atrial fibrillation," *Basic Research in Cardiology*, vol. 101, no. 3, pp. 261–267, 2006.
- [29] H. Cao and S. Y. Xu, "EDC/NHS-crosslinked type II collagen-chondroitin sulfate scaffold: characterization and in vitro evaluation," *Journal of Materials Science*, vol. 19, no. 2, pp. 567–575, 2008.
- [30] H. C. Liang, Y. Chang, C. K. Hsu, M. H. Lee, and H. W. Sung, "Effects of crosslinking degree of an acellular biological tissue on its tissue regeneration pattern," *Biomaterials*, vol. 25, no. 17, pp. 3541–3552, 2004.
- [31] H. W. Sung, R. N. Huang, L. L. H. Huang, and C. C. Tsai, "In vitro evaluation of cytotoxicity of a naturally occurring cross-linking reagent for biological tissue fixation," *Journal of Biomaterials Science, Polymer Edition*, vol. 10, no. 1, pp. 63–78, 1999.
- [32] Y. Chang, C. K. Hsu, H. J. Wei et al., "Cell-free xenogenic vascular grafts fixed with glutaraldehyde or genipin: in vitro and in vivo studies," *Journal of Biotechnology*, vol. 120, no. 2, pp. 207–219, 2005.
- [33] S. F. Badylak, "The extracellular matrix as a scaffold for tissue reconstruction," *Seminars in Cell and Developmental Biology*, vol. 13, no. 5, pp. 377–383, 2002.
- [34] A. D. Bhrany, C. J. Lien, B. L. Beckstead et al., "Crosslinking of an oesophagus acellular matrix tissue scaffold," *Journal of Tissue Engineering and Regenerative Medicine*, vol. 2, no. 6, pp. 365–372, 2008.
- [35] D. W. Courtman, B. F. Errett, and G. J. Wilson, "The role of cross-linking in modification of the immune response elicited against xenogenic vascular acellular matrices," *Journal of Biomedical Materials Research*, vol. 55, no. 4, pp. 576–586, 2001.
- [36] R. Lull, "Immune considerations in tissue engineering," *Clinics in Plastic Surgery*, vol. 26, no. 4, pp. 549–568, 1999.
- [37] M. Dahm, W. D. Lyman, A. B. Schwell, S. M. Factor, and R. W. M. Frater, "Immunogenicity of glutaraldehyde-tanned bovine pericardium," *Journal of Thoracic and Cardiovascular Surgery*, vol. 99, no. 6, pp. 1082–1090, 1990.
- [38] N. Higashi-Kuwata, M. Jinnin, T. Makino, S. Fukushima, Y. Inoue, and F. C. Muchemwa, "Characterization of monocyte/macrophage subsets in the skin and peripheral blood derived from patients with systemic sclerosis," *Arthritis Research & Therapy*, vol. 12, no. 4, article R128, 2010.
- [39] E. G. Lima, A. R. Tan, T. Tai et al., "Genipin enhances the mechanical properties of tissue-engineered cartilage and protects against inflammatory degradation when used as a medium supplement," *Journal of Biomedical Materials Research - Part A*, vol. 91, no. 3, pp. 692–700, 2009.
- [40] S. K. Moestrup and H. J. Moller, "CD163: a regulated hemoglobin scavenger receptor with a role in the anti-inflammatory response," *Annals of Medicine*, vol. 36, no. 5, pp. 347–354, 2004.
- [41] T. K. O'Brien, S. Gabbay, A. C. Parkes, R. A. Knight, and P. J. Zalesky, "Immunological reactivity to a new glutaraldehyde tanned bovine pericardial heart valve," *Transactions of the American Society for Artificial Internal Organs*, vol. 30, pp. 440–444, 1984.
- [42] S. F. Badylak, "The extracellular matrix as a biologic scaffold material," *Biomaterials*, vol. 28, no. 25, pp. 3587–3593, 2007.
- [43] T. W. Gilbert, J. M. Freund, and S. F. Badylak, "Quantification of DNA in Biologic Scaffold Materials," *Journal of Surgical Research*, vol. 152, no. 1, pp. 135–139, 2009.
- [44] P. B. Van Wachem, M. J. A. Van Luyn, L. H. H. O. Damink, P. J. Dijkstra, J. Feijen, and P. Nieuwenhuis, "Tissue regenerating capacity of carbodiimide-crosslinked dermal sheep collagen during repair of the abdominal wall," *International Journal of Artificial Organs*, vol. 17, no. 4, pp. 230–239, 1994.
- [45] H.-W. Sung, W.-H. Chang, C.-Y. Ma, and M.-H. Lee, "Cross-linking of biological tissues using genipin and/or carbodiimide," *Journal of Biomedical Materials Research A*, vol. 64, no. 3, pp. 427–438, 2003.
- [46] S. F. Badylak, J. E. Valentin, A. K. Ravindra, G. P. McCabe, and A. M. Stewart-Akers, "Macrophage phenotype as a determinant of biologic scaffold remodeling," *Tissue Engineering Part A*, vol. 14, no. 11, pp. 1835–1842, 2008.
- [47] M. Rafat, F. Li, P. Fagerholm et al., "PEG-stabilized carbodiimide crosslinked collagen-chitosan hydrogels for corneal tissue engineering," *Biomaterials*, vol. 29, no. 29, pp. 3960–3972, 2008.
- [48] M. E. Nimni, D. Cheung, B. Strates, M. Kodama, and K. Sheikh, "Chemically modified collagen: a natural biomaterial for tissue replacement," *Journal of Biomedical Materials Research*, vol. 21, no. 6, pp. 741–771, 1987.
- [49] C. E. Schmidt and J. M. Baier, "Acellular vascular tissues: natural biomaterials for tissue repair and tissue engineering," *Biomaterials*, vol. 21, no. 22, pp. 2215–2231, 2000.
- [50] E. Gendler, S. Gendler, and M. E. Nimni, "Toxic reactions evoked by glutaraldehyde-fixed pericardium and cardiac valve tissue bioprosthesis," *Journal of Biomedical Materials Research*, vol. 18, no. 7, pp. 727–736, 1984.
- [51] E. Jorge-Herrero, C. Fonseca, A. P. Barge et al., "Biocompatibility and calcification of bovine pericardium employed for the construction of cardiac bioprostheses treated with different chemical crosslink methods," *Artificial Organs*, vol. 34, no. 5, pp. E168–E176, 2010.
- [52] L. L. Huang, H. W. Sung, C. C. Tsai, and D. M. Huang, "Biocompatibility study of a biological tissue fixed with a naturally occurring cross-linking reagent," *Journal of Biomedical Materials Research*, vol. 42, no. 4, pp. 568–576, 1998.
- [53] J. J. Tomasek, G. Gabbiani, B. Hinz, C. Chaponnier, and R. A. Brown, "Myofibroblasts and mechano-regulation of connective tissue remodelling," *Nature Reviews Molecular Cell Biology*, vol. 3, no. 5, pp. 349–363, 2002.